SECOND EUROPEAN CONFERENCE ON EARTHQUAKE ENGINEERING
AND SEISMOLOGY, ISTANBUL AUG. 25-29, 2014

DISPLACEMENT-BASED SEISMIC DESIGN OF DAMPED BRACES FOR RETROFITTING IN-PLAN IRREGULAR FRAMED STRUCTURES

Fabio MAZZA[1] and Tommaso BUCCAFURNI[2]

ABSTRACT

A Displacement-Based Design procedure is proposed for proportioning hysteretic damped braces (HYDBs) in order to attain, for the in-plan least seismic capacity direction and a specific level of seismic intensity, a designated performance level of a reinforced concrete (r.c.) irregular framed building to be retrofitted. To this end, a computer code for the nonlinear static analysis of spatial frames is developed to obtain the pushover curve for an assigned in-plan direction of the seismic loads. The town hall of Spilinga (Italy), a two-storey r.c. framed structure with an L-shaped plan built at the beginning of the 1960s, has been considered as case study. Four alternative structural solutions are examined, derived from the first one by the insertion of HYDBs, considering: the extended N2 method (i.e. case 1) and the extended pushover analysis (i.e. case 2) combined with a proportional (i.e. subcase A) and an inversely proportional (i.e. subcase B) in-plan stiffness distributions of HYDBs. To check the effectiveness and reliability of the design procedure, the nonlinear static response of the unbraced and damped braced frames are compared for different in-plan directions of the seismic loads. R.c. frame members are simulated with a lumped plasticity model, including a flat surface modeling of the axial load-biaxial bending moment elastic domain, while the behaviour of a HYDB is idealized through the use of a bilinear law. Vulnerability index domains are used to estimate the directions of least seismic capacity at the ultimate (i.e. life-safety and collapse prevention) limit states prescribed by Italian and European seismic codes.

INTRODUCTION

Existing framed buildings that have an asymmetrical plan, in order to comply with architectural and functional requirements, have been one of the most frequently damaged type of structures during recent earthquakes. Traditional retrofitting techniques for framed structures are based on the widespread strengthening of the structure and/or on the introduction of additional, very stiff, structural members. In recent decades, innovative strategies for the passive control of framed structures have been experimented, such as those based on the insertion of damped braces, connecting two consecutive stories and incorporating energy dissipating devices (e.g. see Christopoulos and Filiatrault, 2006). The application of such devices to existing buildings is rapidly increasing throughout the world. Several types of both passive and semi-active energy dissipating systems are in use today and many new solutions are being proposed and investigated. The supplementary damping devices can be classified as: displacement-dependent (e.g. hysteretic damper, HYD), velocity-

[1] Researcher, Dipartimento di Ingegneria Civile, Università della Calabria, Rende (Cosenza), Italy, fabio.mazza@unical.it
[2] Research fellow, Dipartimento di Ingegneria Civile, Università della Calabria, Rende (Cosenza), Italy, tommaso.buccafurni@gmail.com

dependent (e.g. viscoelastic damper, VED) and self-centring (e.g. shape memory alloy damper, SMAD). In the present work, attention is focused on metallic yielding hysteretic dampers (HYDs).

For a widespread application of hysteretic damped braces (HYDBs) practical and reliable design procedures are needed. New seismic codes only implicitly allow for the use of these devices (e.g. European code, EC8 2003; Italian code, NTC08 2008), while very few codes across the world provide simplified design criteria (e.g. USA code, FEMA 356 2000). According to the new philosophy of Performance-Based-Design (PBD), a design objective is obtained by coupling a performance level (e.g. operational, immediate occupancy, life-safety or collapse prevention) with a specific level of ground motion intensity (e.g. frequent, occasional, rare or very rare). On the basis of the PBD (Priestley et al., 2007), several simplified nonlinear methods have been proposed, combining the nonlinear static (pushover) analysis of the multi-degree-of-freedom model of the actual structure with the response spectrum analysis of an equivalent single-degree-of-freedom system (Fajfar, 1999). More specifically, two alternative approaches have been followed: (a) the Force-Based Design (FBD) approach combined with required deformation target verification (e.g. see Ponzo et al., 2012); (b) the Displacement-Based Design (DBD) approach, in which the design starts from a target deformation (e.g. see Mazza and Vulcano, 2013) of an equivalent elastic (linear) system with effective properties (i.e. secant stiffness and equivalent viscous damping).

In this paper, the DBD procedure proposed by Mazza and Vulcano (2013), which aims to proportion hysteretic damped braces (HYDBs) so as to attain a designated performance level of an existing framed structure with a symmetric plan (for a specific level of seismic intensity), is extended to in-plan irregular reinforced concrete (r.c.) framed buildings.

NONLINEAR STATIC ANALYSIS OF R.C. FRAMED STRUCTURES

A path-following procedure is considered for the nonlinear static analysis of a r.c. spatial framed structure subjected, besides the gravity loads, to monotonically increasing horizontal (seismic) loads applied in the center of mass (C_M) of each storey along an assigned direction in plan defined by the angle γ (Figure 1). At each step of the analysis, the static equilibrium equations is expressed as

$$\boldsymbol{f}[\boldsymbol{u}] - \boldsymbol{p}(\alpha) = 0 \tag{1}$$

corresponding to an implicit nonlinear system in the unknown displacement vector $\boldsymbol{u}$, where $\boldsymbol{f}$ represents the structural reaction vector and $\boldsymbol{p}$ the external load vector

$$\boldsymbol{p} = \alpha\, \hat{\boldsymbol{p}} \tag{2}$$

α being the load multiplier. In order to avoid convergence problems near the ultimate point of the equilibrium path, an arc-length curvilinear abscissa is assumed to define the $\{\boldsymbol{u}, \alpha\}$ sequence through fixed step size $\Delta\xi$ in spite of a load control strategy based on a step load $\Delta\alpha$. This results in an additional unknown parameter α, with the arc-length condition

$$\Delta\boldsymbol{u}^T \bar{\boldsymbol{K}}\, \Delta\boldsymbol{u} + \mu\Delta\alpha^2 = \Delta\xi^2 \tag{3}$$

representing a circumference of radius $\Delta\xi$ and center in the initial point of the step $\{\boldsymbol{u}^{(k)}, \alpha^{(k)}\}$, $\bar{\boldsymbol{K}}$ and μ being suitable metric factors (Figure 1). At each step of the analysis, starting from a trial solution $\{\boldsymbol{u}_j, \alpha_j\}$, corresponding to the value of $\Delta\xi$, the increments $\Delta\boldsymbol{u}_j$ and $\Delta\alpha_j$ are defined by

$$\Delta\boldsymbol{u}_j = \boldsymbol{u}_j - \boldsymbol{u}^{(k)} \;\; ; \;\; \Delta\alpha_j = \alpha_j - \alpha^{(k)} \tag{4a,b}$$

Then, the unknowns $\{\boldsymbol{u}^{(k+1)}, \alpha^{(k+1)}\}$ can be evaluated through the Newton scheme

$$\boldsymbol{u}_{j+1} = \boldsymbol{u}_j + \dot{\boldsymbol{u}}_j \;\; ; \;\; \alpha_{j+1} = \alpha_j + \dot{\alpha}_j \tag{5a,b}$$

As shown in Figure 1, the solution is found by moving along the tangent to the circumference in $\{\boldsymbol{u}_j, \alpha_j\}$, where the iterative corrections $\dot{\boldsymbol{u}}_j$ and $\dot{\alpha}_j$ are obtained as solutions of the linear system

$$\begin{cases} \boldsymbol{r}_j = \boldsymbol{f}\left[\boldsymbol{u}_j\right] - \boldsymbol{p}\left(\alpha_j\right) = 0 \\ \Delta \boldsymbol{u}_j^T \bar{\boldsymbol{K}}\, \dot{\boldsymbol{u}}_j + \mu \Delta\alpha_j \dot{\alpha}_j = 0 \end{cases} \tag{6a,b}$$

The iteration process ends when a suitable measure of the residual equilibrium error $\boldsymbol{r}_j$ (e.g. $\|\boldsymbol{r}_j\|$) becomes less than a prefixed tolerance (e.g. $f_{tol}=10^{-4}$). Further details can be found in a previous work of Mazza (2014).

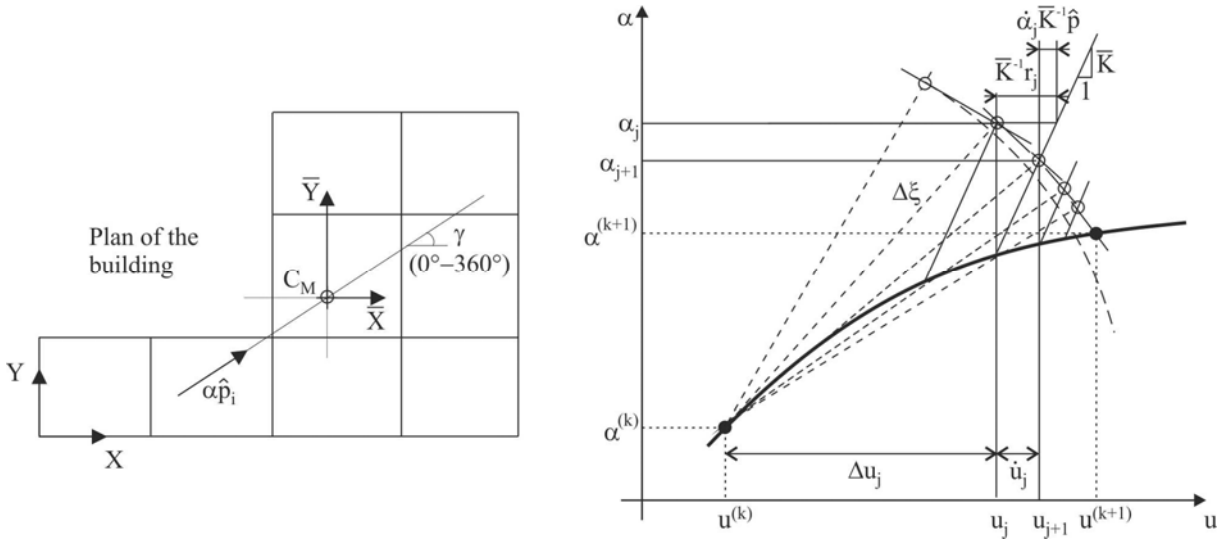

Figure 1. Nonlinear static analysis of r.c framed structure: arc-length iteration scheme

A lumped plasticity model constituted of two parallel elements, one linearly elastic and the other elastic-perfectly plastic, is considered to describe the inelastic behaviour of an r.c. frame member (Mazza and Mazza, 2010). The elastic component is characterized by the flexural stiffness pEI_r, p being the hardening ratio of the moment-curvature law. The elastic-perfectly plastic component exhibits inelastic deformations, lumped at the end cross-sections (i and j), which are determined with reference to an axial force–biaxial bending elastic domain. Torsional strains are assumed to be fully elastic while shear deformations are neglected. Flat surfaces are used to describe the elastic domain, by considering a piecewise linearization of its bounding surface (Mazza and Mazza, 2012). Specifically, a satisfactory representation of the N–M_y–M_z interaction domain has been obtained by considering 26 flat surfaces, including: 6 surfaces normal to the principal axes x, y and z (Figure 2a); 12 surfaces normal to the bisections of the y–z, x–y and x–z principal planes (Figure 2b); 8 surfaces normal to the bisections of the octants (Figure 2c).

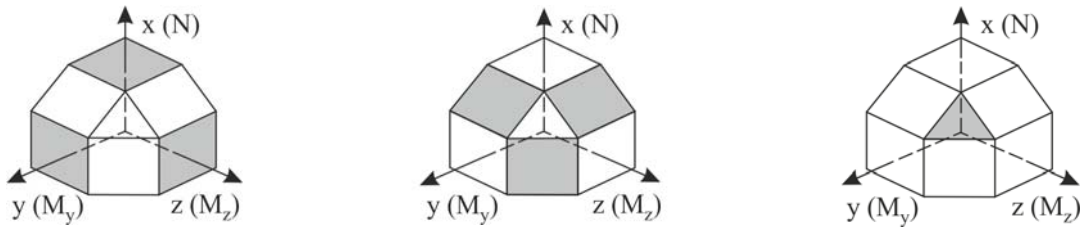

(a) (b) (c)

Figure 2. Flat surfaces approximating the elastic domain of r.c. section

The elastic-plastic solution, represented by point P, is obtained as a projection of the elastic solution, represented by point E, on the active flat surface of the elastic domain (Figure 3a). Otherwise, when the elastic solution lies within the fan limited by the planes normal to the boundaries of the flat surfaces, point P can be located along the active line (Figure 3b) or at the active corner (Figure 3c) resulting from the intersection of these surfaces.

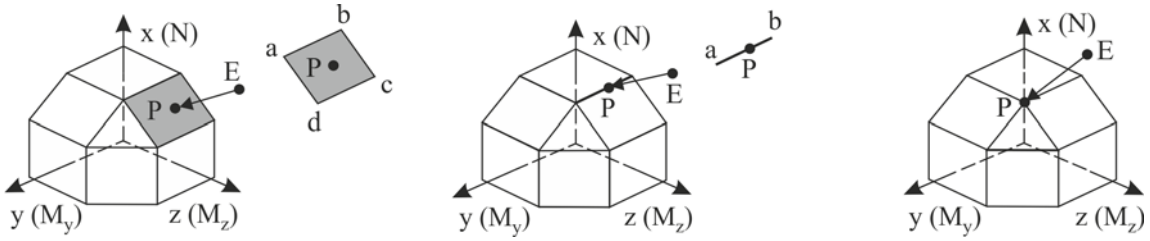

(a) Active flat surface (b) Active line (c) Active corner

Figure 3. Elastic-plastic solution of r.c. frame member

DISPLACEMENT-BASED DESIGN OF HYSTERETIC DAMPED BRACES

A Displacement-Based Design (DBD) procedure proposed by Mazza and Vulcano (2013), which aims to proportion hysteretic damped braces (HYDBs) so as to attain a designated performance level of an existing r.c. framed structure with a symmetric plan (for a specific level of seismic intensity), is extended to in-plan irregular framed buildings. The main steps of the proposed design procedure are summarized below.

1. Extended pushover analysis of the in-plan irregular unbraced frame to obtain base shear and top displacement capacity domains and least seismic capacity direction

Nonlinear static analysis of the in-plan irregular unbraced frame (whose properties are assumed as given), under constant gravity loads and monotonically increasing horizontal loads applied at the centre of mass (C_M) of each storey, is extended to different in-plan directions defined by the angle γ shown in Figure 4a (e.g. increased with a constant step in the range 0-360°). In particular, the aim of the extended pushover analysis is to obtain the lowest base shear ($V_X^{(F)}$-$V_Y^{(F)}$) capacity domain from those corresponding to the most common lateral-load profiles: e.g. a "uniform" distribution, proportional to the floor masses (m_1, m_2, .., m_n); a “triangular” distribution, obtained by multiplying a linear first-mode vibration mode (ϕ_1, ϕ_2, .., ϕ_n) by the corresponding floor masses. Then, the top (roof) displacement (d_X-d_Y) capacity domain is evaluated. Finally, the $V_\gamma^{(F)}$-d_γ curve in the least seismic capacity direction is selected with reference to the maximum value of the vulnerability index

$$VI = d_{D,\gamma}^{(ls)} \Big/ d_{C,\gamma}^{(ls)} \tag{7}$$

defined as the ratio between the maximum displacement demand ($d_{D,\gamma}^{(ls)}$), to an arbitrary corner in the building plan, and the corresponding capacity ($d_{C,\gamma}^{(ls)}$) at the ultimate (i.e. life-safety, LS, or collapse prevention, CP) limit state (ls).

2. Definition of an equivalent single degree of freedom (ESDOF) system in the least seismic capacity direction to evaluate the equivalent viscous damping due to hysteresis

The selected $V_\gamma^{(F)}$-d_γ curve can be idealized as bilinear and the original frame can be represented by an ESDOF system (Fajfar, 1999) characterized by a bilinear curve (V_γ^*-d_γ^*), with a yield displacement $d_{y,\gamma}^{(F)}$ and a stiffness hardening ratio r_F, derived from the idealized $V_\gamma^{(F)}$-d_γ curve (see Figure 4b). Once the displacement ($d_{p,\gamma}$) and the corresponding base shear ($V_{p,\gamma}^{(F)}$) are settled, for a given performance level, the ductility

$$\mu_{F,\gamma} = d_{p,\gamma} \Big/ d_{y,\gamma}^{(F)} \tag{8}$$

and the equivalent (secant) stiffness

$$K_{e,\gamma}^{(F)} = V_{p,\gamma}^{(F)} \Big/ d_{p,\gamma} \tag{9}$$

can be evaluated for the frame.

As a preliminary estimation of the equivalent viscous (biaxial) damping due to hysteresis of the framed structure ($\xi_{F,\gamma}^{(h)}$), an expression derived from experimental results carried out on r.c. frame

members subjected to axial load and biaxial bending is considered (Rodrigues et al., 2012)

$$\xi_{F,\gamma}^{(h)}(\%)=12.56+5.18ln\left(\mu_{F,\gamma}\right) \tag{10}$$

where $\mu_{F,\gamma}$ is defined above.

3. Equivalent viscous damping due to hysteresis of the damped braces

If the constitutive law of the equivalent damped brace is idealized as bilinear (see Figure 4c), the corresponding viscous damping (ξ_{DB}) can be evaluated as (Rosenblueth and Herrera, 1964)

$$\xi_{DB}(\%)=63.7\left(\mu_{DB}-1\right)\left(1-r_{DB}\right)\Big/\left[\mu_{DB}+\mu_{DB}r_{DB}\left(\mu_{DB}-1\right)\right] \tag{11}$$

where

$$\mu_{DB}=\left[1+\left(\mu_D-1\right)\left(1+r_DK_D^*\right)\right]\Big/\left(1+K_D^*\right) \tag{12}$$

and

$$r_{DB}=\left(1/K_B+1/K_D\right)\Big/\left[1/K_B+1/\left(r_DK_D\right)\right]=r_D\left(1+K_D^*\right)\Big/\left(1+r_DK_D^*\right) \tag{13}$$

are the ductility demand and the stiffness hardening ratio of the equivalent damped brace, respectively. Moreover, μ_D represents the damper ductility, whose value should be compatible with the deformation capacity of the damper itself, r_D the stiffness hardening ratio of the damper and $K^*_D(=K_D/K_B)$ the stiffness ratio reasonably assumed as rather less than 1. Finally, the stiffness of a damped brace (K_{DB}) can be expressed as for an in-series system depending on the brace stiffness (K_B) and the elastic stiffness of the damper (K_D):

$$K_{DB}=1\Big/\left(1/K_B+1/K_D\right) \tag{14}$$

4. Equivalent viscous damping of the damped braced frame in the least seismic capacity direction

Assuming a suitable value of the elastic viscous damping for the framed structure (e.g. ξ_V=5%), the equivalent viscous damping of the in-parallel system comprised of framed structure (F) and damped braces (DBs) is

$$\xi_{e,\gamma}(\%)=\xi_V+\left[\xi_{F,\gamma}^{(h)}V_{p,\gamma}^{(F)}+\xi_{DB}V_{p,\gamma}^{(DB)}\right]\Big/\left[V_{p,\gamma}^{(F)}+V_{p,\gamma}^{(DB)}\right] \tag{15}$$

where $\xi_{F,\gamma}^{(h)}$ and ξ_{DB} have been calculated in steps 2 and 3, respectively, $V_{p,\gamma}^{(F)}$ has been defined above and $V_{p,\gamma}^{(DB)}$ represents the base-shear contribution due to the damped braces of the damped braced frame at the performance point (Figure 4c). Then, with reference to the displacement spectrum for $\xi_{e,\gamma}$, the effective period ($T_{e,\gamma}$) of the DBF can be evaluated as the period corresponding to the performance displacement $d_{p,\gamma}$.

5. Effective stiffness of the equivalent damped brace in the least seismic capacity direction

Once the mass of the ESDOF system, $m_e=\sum m_i\phi_i$, is calculated, the effective stiffness of DBF ($K_{e,\gamma}$) and the effective stiffness required by the damped braces ($K_{e,\gamma}^{(DB)}$) can be evaluated as

$$K_{e,\gamma}=4\pi^2m_e\Big/T_{e,\gamma}^2 \tag{16}$$

$$K_{e,\gamma}^{(DB)}=K_{e,\gamma}-K_{e,\gamma}^{(F)} \tag{17}$$

6. Effective strength properties of the equivalent damped brace in the least seismic capacity direction

Because the base shear-displacement curve representing the response of the damped braces of the actual structure ($V_\gamma^{(DB)}$-d_γ) has been idealized as bilinear, the base-shear contributions of the damped braces at the performance and yielding points ($V_{p,\gamma}^{(DB)}$ and $V_{y,\gamma}^{(DB)}$, respectively) can be calculated as:

$$V_{p,\gamma}^{(DB)}=K_{e,\gamma}^{(DB)}d_{p,\gamma} \tag{18}$$

$$V_{y,\gamma}^{(DB)} = V_{p,\gamma}^{(DB)} \Big/ \left[1 + r_{DB}\left(\mu_{DB} - 1\right)\right] \tag{19}$$

It is worth mentioning that the equivalent viscous damping expressed by Eq. (15) depends on the base-shear $V_{p,\gamma}^{(DB)}$, which is initially unknown. As a consequence, an iterative procedure is needed for the solution of Eqs. (15)–(19).

7. Design of the hysteretic damped braces of the damped braced frame (DBF)

The in-elevation distribution of the lateral loads carried by the HYDBs at the yielding point ($d_{y,\gamma}^{(DB)}$) can be assumed. In particular, once the shear at the i^{th} storey is calculated

$$V_{yi,\gamma}^{(DB)} = \sum_{j=i}^{n} F_{yj,\gamma}^{(DB)} = \sum_{j=i}^{n} \frac{m_j \phi_j}{\sum_{k=1}^{n} m_k \phi_k} V_{y,\gamma}^{(DB)} \tag{20}$$

the corresponding elastic (lateral) stiffness of the damped braces in the γ direction of least seismic capacity is expressed as

$$K_{i,\gamma}^{(DB)} = \frac{V_{yi,\gamma}^{(DB)}}{\left(\phi_i - \phi_{i-1}\right) d_{y,\gamma}^{(DB)}} \tag{21}$$

Then, two different criteria are followed for distributing the stiffness properties of the HYDBs in-plan, obtained at each storey, among the single damped braces placed in the X (i.e. $K_X^{(DB)}$) and Y (i.e. $K_Y^{(DB)}$) plane frames (e.g. in the perimeter frames highlighted in Figure 4d): a proportional stiffness criterion, which assumes the same position of the centre of stiffness for the unbraced ($C_S^{(UF)}$) and damped braced ($C_S^{(DBF)}$) frames (i.e. assuming $e_X^{(DBF)}=e_X^{(UF)}$ and $e_Y^{(DBF)}=e_Y^{(UF)}$), in order to obtain modal shapes of the structure practically unchanged after the insertion of HYDBs; an inversely proportional stiffness criterion, which considers a position of $C_S^{(DBF)}$ equal to that of C_M (i.e. assuming $e_X^{(DBF)}=e_Y^{(DBF)}=0$), in order to eliminate (elastic) torsional effects. Strength distribution of HYDBs is assumed to be proportional to the stiffness distribution.

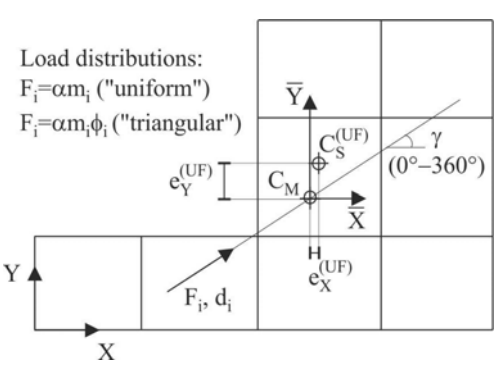

(a) In-plan irregular unbraced frame (UF)

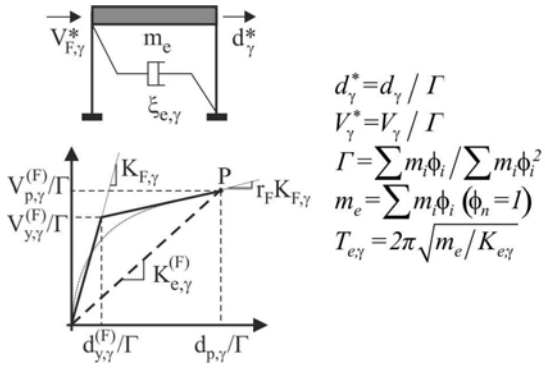

(b) ESDOF of the framed structure (F)

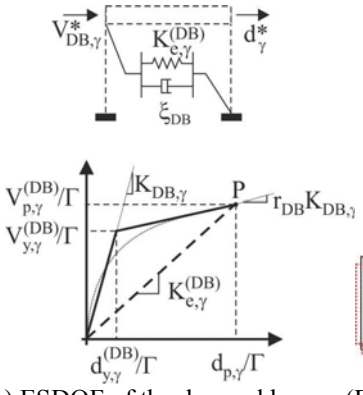

(c) ESDOF of the damped braces (DBs)

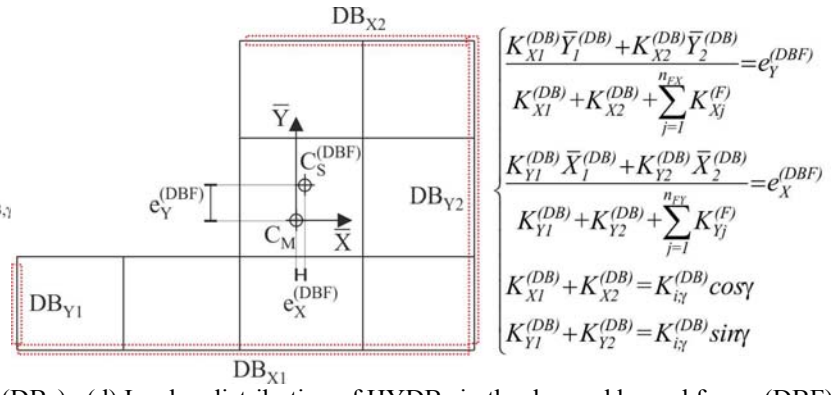

(d) In-plan distribution of HYDBs in the damped braced frame (DBF)

Figure 4. Quantities for designing hysteretic damped braces (HYDBs)

LAYOUT AND DESIGN OF THE TEST STRUCTURE

The town hall of Spilinga (Figure 5a), a small town near Vibo Valentia (Italy), is considered as a reference for the numerical investigation. This two-storey r.c. framed structure, with an L-shaped plan (Figure 5b), was built at the beginning of the 1960s. The structure was designed to comply with the admissible tension method, according to the Italian seismic code in force at the time of construction (Royal Decree-Law, R.D.L., 1935), for a high-risk seismic region (degree of seismicity S=12, which corresponds to a coefficient of seismic intensity C=0.10) and a medium subsoil class (R.D.L. 1937). Steel properties were estimated according to the Italian standards (R.D.L. 1939); namely, since the Aq60 steel was used, a yield strength of 310 MPa was assumed.

The gravity loads are represented by dead and live loads, whose values are, respectively, equal to: 5.1 kN/m^2 and 3 kN/m^2, on the first floor; 3.9 kN/m^2 (including also the weight of the roof) and 0.5 kN/m^2, on the second floor. The contribution of the masonry-infills, made with two layers of full bricks with a thickness of 0.12 m each, is taken into account by considering a weight of 2.7 kN/m^2. The total mass of the building is assumed equal to 458 kNs^2/m, subdivided between 268 kNs^2/m and 190 kNs^2/m on the first and second floor, respectively. To improve the knowledge level of the Spilinga building the present work uses a simulated design (Mazza, 2014), with reference to the codes in force at the time of construction. The strengths of concrete and steel have been divided by a confidence factor equal to 1.2 corresponding to a normal level of knowledge, according to NTC08.

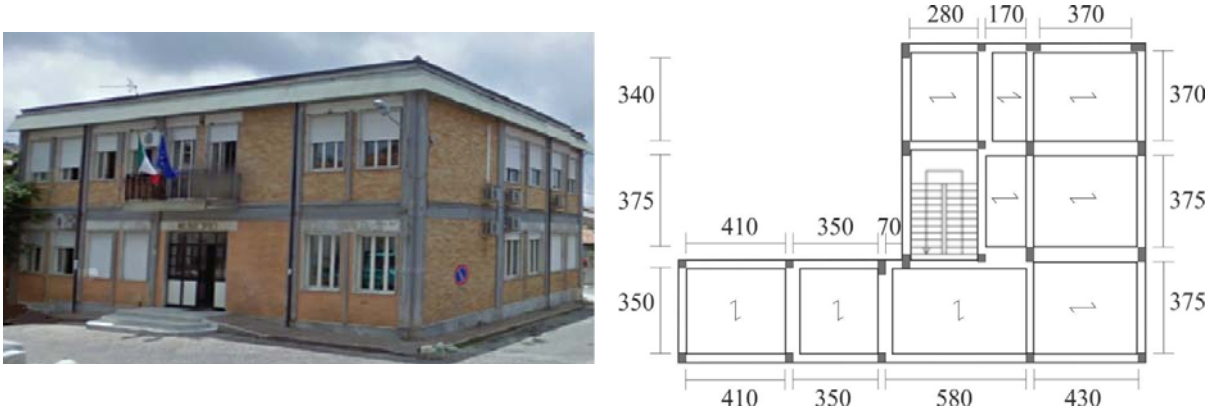

(a) Current state (b) Plan (dimensions in cm)

Figure 5. Town hall of Spilinga (Vibo Valentia, Italy)

For the purpose of retrofitting the original structure to the provisions imposed by NTC08 and EC8, assuming a high-risk seismic region and soft subsoil class, diagonal steel braces equipped with HYDs are inserted. HYDBs are placed along the in-plan principal directions, at both storeys, in the perimeter plane frames only (Figure 6). In order to evaluate the higher mode torsional effects, basic pushover analysis along the in-plan principal (i.e. X and Y) directions of the structure and standard elastic modal analysis are combined according to the extended N2 method (Kreslin and Fajfar, 2012). Displacement correction factors are evaluated by considering the ratio between the normalized roof displacements obtained by elastic modal analysis and basic pushover analysis. The normalized roof displacement is defined as the roof displacement at an arbitrary in-plan location divided by the corresponding value at the centre of mass (C_M).

Four alternative structural solutions are examined, considering both the extended N2 method (i.e. case 1) and the extended pushover method carried out along different in-plan directions of the horizontal loads in the range 0°-360° (i.e. case 2), combined with the proportional (i.e. subcase A, Figure 6a) and the inversely proportional (i.e. subcase B, Figure 6b) in-plan stiffness distributions of HYDBs. The position of the mass and stiffness centres on the first (i.e. $C_{M,1}$ and $C_{S,1}$) and second (i.e. $C_{M,2}$ and $C_{S,2}$) floors are also plotted in Figure 6. In particular, to avoid brittle behaviour of the r.c. structure, a design value of the frame ductility μ_F=1.2=1.0*γ_{SLV}, where e.g. a safety factor γ_{SLV}=1.2, is considered at the life-safety (LS) limit state; moreover, a design value of the damper ductility μ_D=10 and a hardening ratio r_D=5% are assumed. In-plan and in-elevation distribution laws of the lateral stiffness (i.e. $K_i^{(DB)}$) and yield-load (i.e. $V_{yi}^{(DB)}$) are reported in Table 1, assuming the design direction

γ=120° in the structural solutions 2.A and 2.B. Strength distribution of the HYDBs is taken as proportional to the stiffness distribution. It is worth noting that the lateral stiffness of the damped brace (K_{DB}) is assumed equal to the lateral stiffness of the damper (K_D), given that the brace is much stiffer than the damper which it supports (i.e. $K_B \rightarrow \infty$).

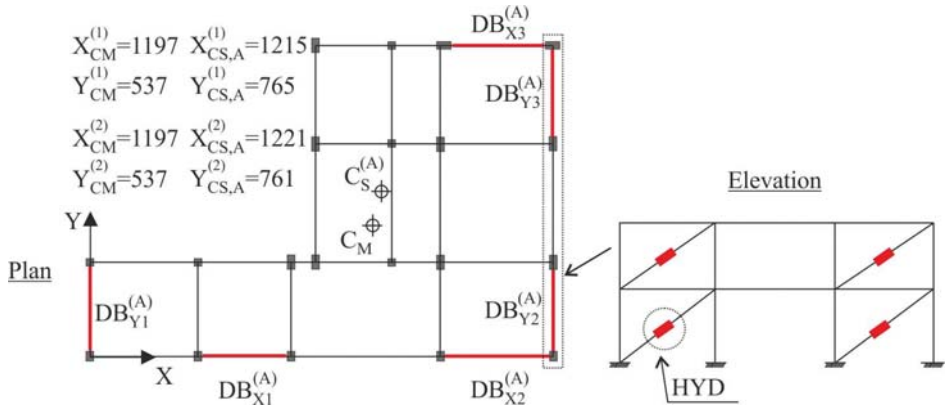

(a) Subcase A: proportional stiffness criterion

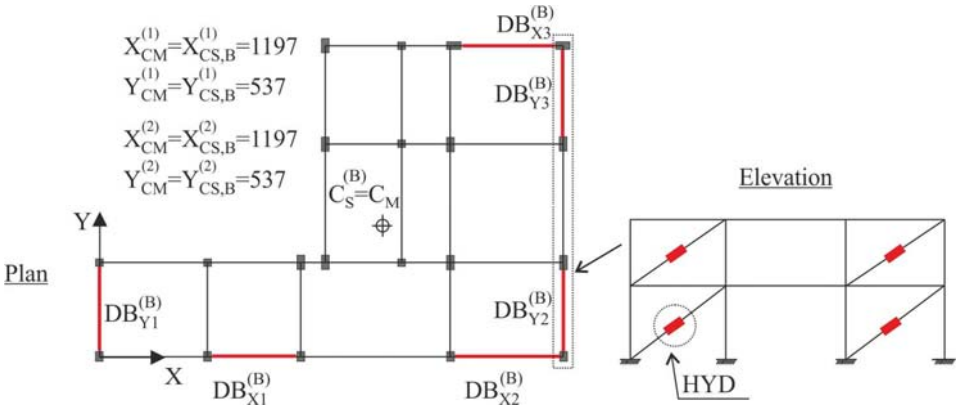

(b) Subcase B: inversely proportional stiffness criterion

Figure 6. In-plan and in-elevation distributions of HYDBs (dimensions in cm)

Table 1. Stiffness and strength properties of the HYDBs

case 1.A	$K_i^{(DB)}$ (kN/m)						$V_{yi}^{(DB)}$ (kN)					
Storey	X_1	X_2	X_3	Y_1	Y_2	Y_3	X_1	X_2	X_3	Y_1	Y_2	Y_3
2	132078	132078	387063	299797	81403	81403	81	81	240	224	61	61
1	220564	220564	648299	506745	139297	139297	143	143	417	389	107	107
case 1.B	$K_i^{(DB)}$ (kN/m)						$V_{yi}^{(DB)}$ (kN)					
Storey	X_1	X_2	X_3	Y_1	Y_2	Y_3	X_1	X_2	X_3	Y_1	Y_2	Y_3
2	246412	246412	171625	281398	90459	90459	149	149	104	210	68	68
1	371346	371346	367101	492022	146477	146477	236	236	232	378	112	112
case 2.A	$K_i^{(DB)}$ (kN/m)						$V_{yi}^{(DB)}$ (kN)					
Storey	X_1	X_2	X_3	Y_1	Y_2	Y_3	X_1	X_2	X_3	Y_1	Y_2	Y_3
2	63882	63882	187210	382371	103824	103824	77	77	224	242	66	66
1	106680	106680	313562	646317	177664	177664	133	133	389	421	116	116
case 2.B	$K_i^{(DB)}$ (kN/m)						$V_{yi}^{(DB)}$ (kN)					
Storey	X_1	X_2	X_3	Y_1	Y_2	Y_3	X_1	X_2	X_3	Y_1	Y_2	Y_3
2	144090	144090	36168	362428	113707	113707	166	166	42	230	72	72
1	199063	199063	141409	629662	185905	185905	242	242	171	410	122	122

NUMERICAL RESULTS

To check the effectiveness and reliability of the proposed DBD procedure for retrofitting in-plan irregular framed structures, the nonlinear static response of the Spilinga building is carried out for

different in-plan directions of the seismic loads defined by the angle γ (increased in the range 0-360° with a constant step of 15°). A lumped plasticity model, including a piecewise linearization of the axial load-biaxial bending moment elastic domain of the cross-sections, is considered for the r.c. frame members while the behaviour of a HYDB is idealized through the use of a bilinear law. A vulnerability index (see Eq. (7)) is evaluated at the life-safety (LS) and collapse prevention (CP) ultimate limit states prescribed by NTC08 and EC8. The LS and CP limit states are reached when a ductile mechanism at the member level, in terms of chord-rotation (NTC08), or a brittle mechanism at the section level, in terms of shear force (EC8), is attained. In particular, the LS ductile and brittle thresholds are assumed equal to ¾ of the corresponding CP ultimate values. The bi-directionality of the horizontal seismic loads and the in-plan irregularity of the structural configuration can induce bi-directional chord rotations and shear forces which are also taken into account (Mazza, 2014).

Firstly, the numerical results obtained by considering the DBD procedure in conjunction with the extended N2 (i.e. case 1) and extended pushover (i.e. case 2) methods, assuming the proportional (i.e. subcase A) and inversely proportional (i.e. subcase B) criteria for the in-plan stiffness distribution of HYDBs, are plotted in Figure 7.

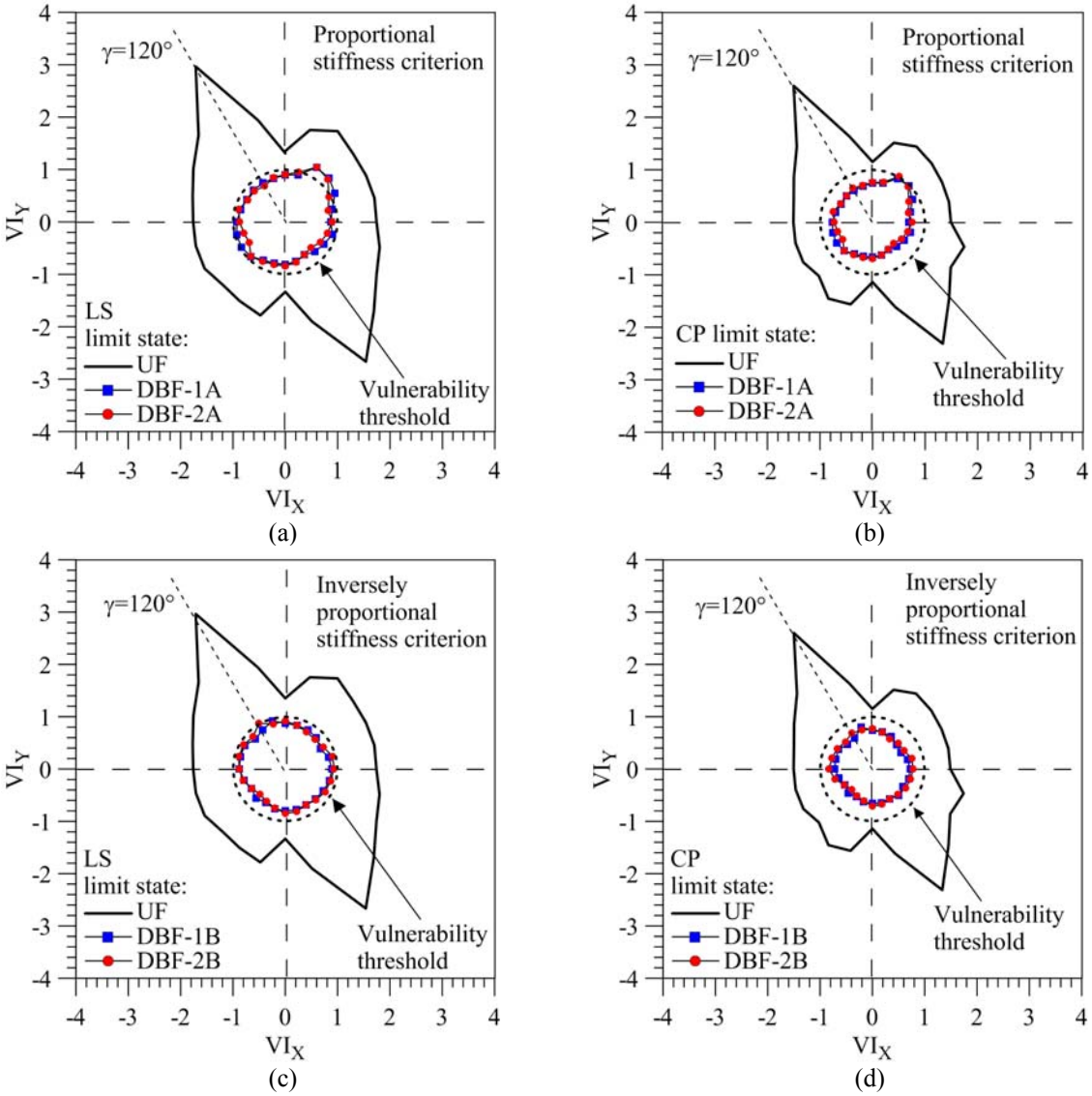

Figure 7. Comparisons of results obtained for the unbraced (UF) and damped brace (DBF) frames: extended N2 (DBF-1) and extended pushover (DBF-2) methods with proportional (A) and inversely proportional (B) stiffness criteria

In particular, the maximum value of the vulnerability index (VI), corresponding to an arbitrary corner in the building plan, has been evaluated by rotating the direction of the seismic loads by the

angle γ (in the range 0-360° with a constant step of 15°); a "triangular" load distribution has been assumed. As can be observed, the unbraced frame (UF) has exceeded the vulnerability threshold for all directions of the seismic loads, showing an irregular shape of the corresponding vulnerability index domains. The insertion of HYDBs (i.e. the damped braced frames, DBF-1A and DBF-2A structures) proved to be favourable, especially at the CP limit state (Figures 7b,d) and in the case of the inversely proportional stiffness criterion (Figures 7c,d), confirming the effectiveness of their design carried for limiting the local damage suffered by the r.c. frame members. It is worth noting that the most vulnerable directions, at the LS and CP limit states, are not necessarily the same for the extended N2 (i.e. the DBF-1A and DBF-1B structures) and extended pushover (i.e. the DBF-2A and DBF-2B structures) methods. Moreover, similar curves have been obtained for the DBF-1A and DBF-2A structures (Figures 7a,b) and the DBF-1B and DBF-2B structures (Figures 7c,d) for each limit state, respectively. This kind of behaviour confirms that the extended N2 method is able to provide a reasonable prediction of higher mode torsional effects thereby obviating the computational effort of the extended pushover analysis.

Curves analogous to the previous ones are shown in Figure 8 to compare the proportional (A) and inversely proportional (B) criteria for the in-plan stiffness distribution of HYDBs, with reference to the extended N2 (Figures 8a,b) and extended pushover (Figures 8c,d) methods.

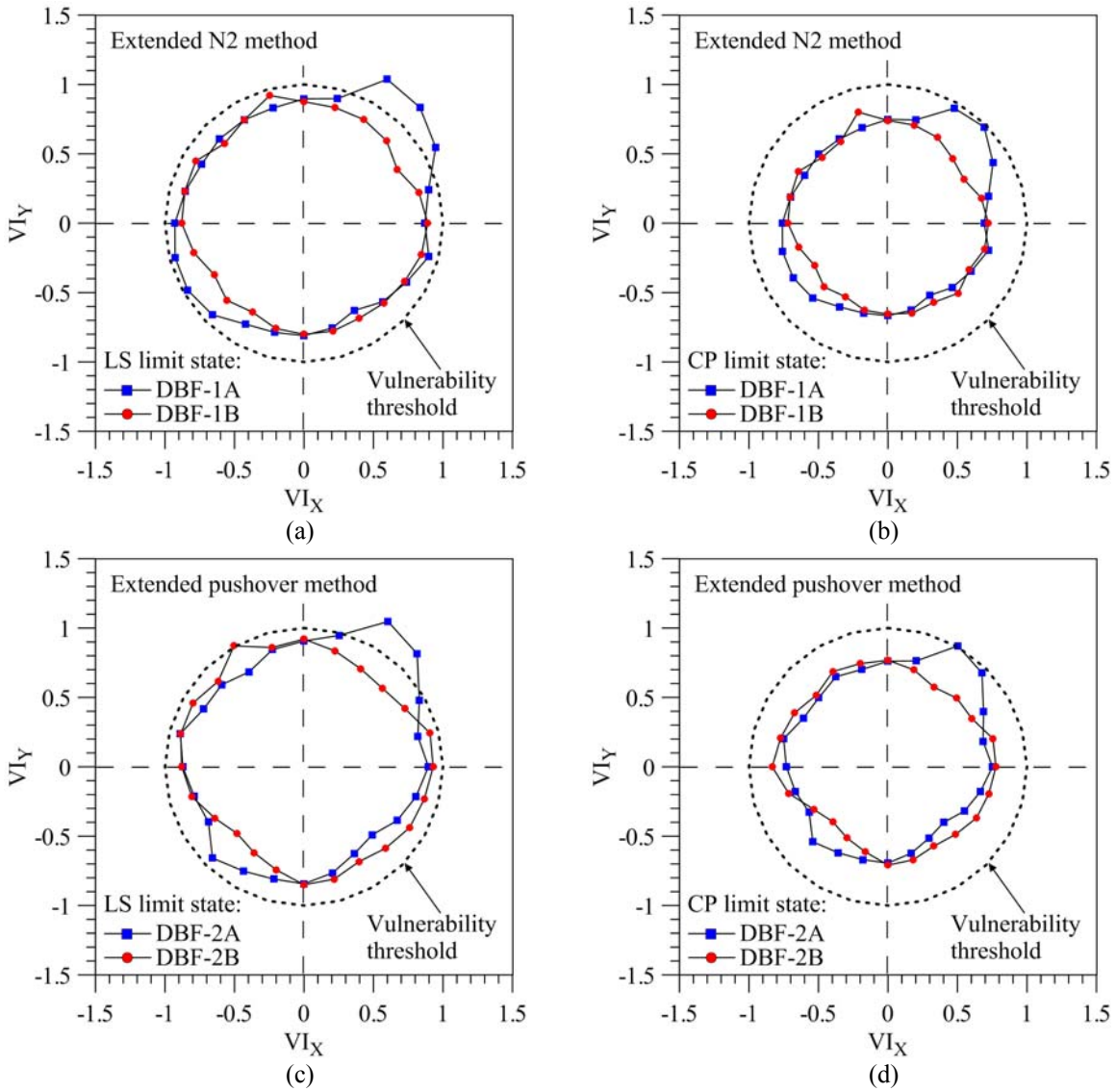

Figure 8. Comparisons of results obtained for the damped brace frames (DBFs): proportional (A) and inversely proportional (B) stiffness criteria with extended N2 (DBF-1) and extended pushover (DBF-2) methods

As can be observed, the effectiveness of the inversely proportional stiffness distribution of the HYDBs is generally found to be better than that observed for the proportional stiffness distribution, both at the LS (Figures 8a,c) and CP (Figures 8b,d) ultimate limit states, with a vulnerability threshold not reached for any of the in-plan directions of the seismic loads. The shape of the vulnerability domains obtained for the DBF-1B and DBF-2B structures proved to be more regular than that observed for the DBF-1A and DBF-2A structures, respectively. Moreover, the most vulnerable seismic directions at the LS and CP limits states are not necessarily the same for the above mentioned criteria.

Finally, minimum and maximum values of the vulnerability index in the damped braced frames, selected from those obtained for the in-plan corners, are compared at the LS limit state (Figure 9). More precisely, the inelastic torsional effects obtained by considering the extended N2 (Figures 9a,b) and extended pushover (Figures 9c,d) methods, with proportional (A) and inversely proportional (B) stiffness distributions of the HYDBs, are investigated. As expected, differences are found in the DBF-1A (Figure 9a) and DBF-2A (Figure 9c) structures which assume the same position of the centre of stiffness for the unbraced and damped braced frames. On the other hand, unequal seismic demands on the floor were induced also in the DBF-1B (Figure 9b) and DBF-2B (Figure 9d) structures, because plastic deformations occurred, altough the position of $C_S^{(DBF)}$ equal to that of C_M was assumed in the elastic range.

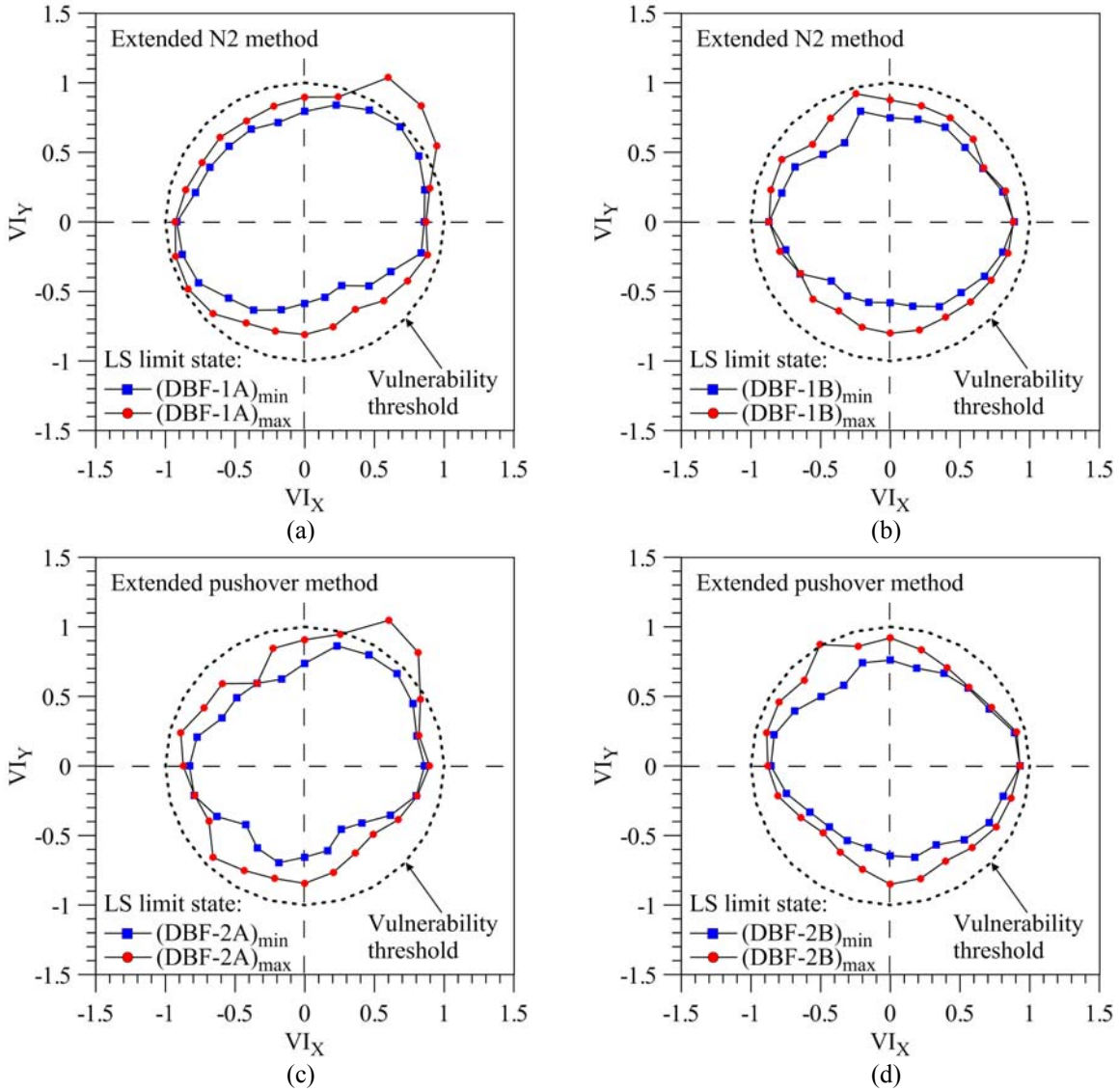

Figure 9. Torsional effects in the damped brace frame (DBF) at the LS limit state: extended N2 (DBF-1) and extended pushover (DBF-2) methods with proportional (A) and inversely proportional (B) criteria

CONCLUSIONS

The results of nonlinear static analyses, carried out on different in-plan directions of the seismic loads in the range 0°-360°, showed the effectiveness of the proposed DBD procedure for proportioning the HYDBs inserted to attain a designated safety level, for an assigned level of seismic intensity, of an in-plan irregular r.c. framed structure. More specifically, the vulnerability levels of the town hall of Spilinga, a small town near Vibo Valentia (Italy), obtained with the extended N2 and the extended pushover methods, were found to be comparable at the ultimate (i.e. LS and CP) limit states provided by NTC08 and EC8. If this result is confirmed through further studies, a reliable DBD procedure of HYDBs, in conjunction with basic pushover analysis along the in-plan principal directions of the structure and standard elastic modal analysis, will become available for practical applications. Moreover, the adoption of the inversely proportional stiffness criterion was found to be preferable to the proportional one for distributing in-plan the stiffness properties of the HYDBs, showing a more regular shape of the vulnerability index domains for different in-plan directions of the seismic loads. Finally, torsional effects highlighted in the unbraced frame are reduced but not eliminated when using both proportional and inversely proportional stiffness criteria in the damped braced frames.

ACKNOWLEDGMENTS

The present work was financed by Re.L.U.I.S. (Italian network of university laboratories of earthquake engineering), "convenzione D.P.C.-Re.L.U.I.S. 2014, Isolation and Dissipation".

REFERENCES

Christopoulos, C and Filiatrault A (2006) Principles of passive supplemental damping and seismic isolation, IUSS Press, Istituto Universitario di Studi Superiori di Pavia (Italy)

Eurocode 8 (2003) Design of structures for earthquake resistance - part 1: general rules, seismic actions and rules for buildings. C.E.N., European Committee for Standardization

Fajfar P (1999) "Capacity spectrum method based on inelastic spectra", *Earthquake Engineering and Structural Dynamics*, 28:979-993

Federal Emergency Management Agency, FEMA 356 (2000) Prestandard and commentary for the seismic rehabilitation of buildings. American Society of Civil Engineers, Reston, Virginia

Kreslin M, Fajfar P (2012) "The extended N2 method considering higher mode effects in both plan and elevation", *Bulletin of Earthquake Engineering*, 10:695-715

Italian Ministry of Infrastructures (2008) "Nuove norme tecniche per le costruzioni e relative istruzioni", D.M.14-01-2008 e Circolare 02-02-2009, n. 617/C.S.LL.PP. (in Italian)

Mazza F (2014) "Modeling and nonlinear static analysis of reinforced concrete framed buildings irregular in plan", submitted to *Engineering Structures*

Mazza F, Mazza M (2010) "Nonlinear analysis of spatial framed structures by a lumped plasticity model based on the Haar–Kàrmàn principle", *Computational Mechanichs*, 45:647-664.

Mazza F, Mazza M (2012) "Nonlinear modeling and analysis of r.c. framed buildings located in a near-fault area", *The Open Construction and Building Technology Journal*, 6:364-372**.**

Mazza F, Vulcano A (2013) "Nonlinear seismic analysis to evaluate the effectiveness of damped braces", *International Journal of Mechanics*, 7(3):251-261

Ponzo FC, Di Cesare A, Nigro D, Vulcano A, Mazza F, Dolce M, Moroni C (2012) "JET-PACS project: dynamic experimental tests and numerical results obtained for a steel frame equipped with hysteretic damped chevron braces", *Journal of Earthquake Engineering*, 16:662-685

Priestley MJN, Calvi GM and Kowalsky MJ (2007) Displacement-based seismic design of structures, IUSS Press, Istituto Universitario di Studi Superiori di Pavia (Italy)

Rodrigues H, Varum H, Arêde A, Costa A (2012) "A comparative analysis of energy dissipation and equivalent viscous damping of RC columns subjected to uniaxial and biaxial loading", *Eng. Structures*, 35:149-164

Rosenblueth E, Herrera I (1964) "On a kind of hysteretic damping", *J. Eng. Mech. Division ASCE*, 90:37–48

Royal Decree-Law No. 2105 (1937) "Technical Building Regulations, with special prescriptions for localities affected by earthquakes" (in Italian)

Royal Decree-Law No. 2229 (1939) "Regulations for the construction of not reinforced and reinforced buildings" (in Italian)

Royal Decree-Law No. 640 (1935) "New text of the Technical Building Regulations, with special prescriptions for localities affected by earthquakes" (in Italian)